Tellus (1988), *40A*, 419–433

In search of a simple scaling for the height of the stratified atmospheric boundary layer

By S. A. KITAIGORODSKII, *Department of Earth and Planetary Sciences, The John Hopkins University, Baltimore, MD 21218, USA* and SYLVAIN M. JOFFRE, *Finnish Meteorological Institute, Air Quality Department, SF-00810 Helsinki, Finland*

(Manuscript received 2 February 1987; in final form 9 February 1988)

ABSTRACT

On the basis of observational data of the atmospheric boundary layer (ABL), a simple scaling framework for the evolving ABL is proposed. The theoretical background is based on a simple parameterization of the vertically-integrated dissipation term in the turbulent kinetic energy equation. The scaling introduces the scaling length $L_N = u_*/N$ where u_* is the friction velocity and N the buoyancy frequency, and it applies to both stable and unstable cases. The scaling fits well 3 different sets of data: the Wangara data, the JASIN data and those from an expedition over the sea ice field of the Baltic Sea. The scaling length related to the rotation appears only as a secondary factor.

1. Introduction

Although much progress has been made in studies of atmospheric boundary layer (ABL) evolution in both the convective (e.g., Tennekes, 1973; Zeman and Tennekes, 1977; Zeman and Lumley, 1976) and mechanical (e.g., Niiler, 1975; Garnich and Kitaigorodskii, 1977, 1978) asymptotic cases, there is still a need for a theoretical and empirical description of the dual case including both types of turbulence production. The mechanically-mixed type of ABL has aroused very little interest so far, although it appears rather frequently with straticform cloudiness and a strong wind over the sea or, in general, during the period of the year when solar radiation is not strong enough to drive a convective ABL (Nicholls and Readings, 1979).

The ABL exhibits a very different regime under nocturnal stably-stratified conditions when buoyancy is a sink of turbulent energy and only wind shear can sustain the turbulence. This type of ABL presents many more problems from both the theoretical (Zeman, 1979) and the observational (Caughey et al., 1979) points of view.

The main result from recent models or observations of an unstably- or stably-stratified ABL is that steady state approaches are generally not relevant, and the one central parameter that describes or monitors the evolution of the ABL is its height h. Knowledge of this height is also very important for many applications, e.g., pollutant diffusion, fog or minimum temperature predictions, trajectory models and the use of similarity laws in numerical weather models. However, under certain conditions, the actual h tends towards an equilibrium value $h^{(e)}$ imposed by the particular structure of the flow. Then the departure of h from $h^{(e)}$ can give a lot of information on the processes driving the ABL dynamics (e.g., Nieuwstadt and Tennekes, 1981).

The classical way of describing the structure of the ABL is by the Kazanski-Monin (1960) type of similarity theory, where the only influencing agents are rotation and buoyancy. It is obvious, however, that other factors should be taken into account. One driving process behind the growth of ABLs is entrainment, the intensity of which is connected with background stratification. Thus, the dynamics of the ABL should be more completely described using this additional physical concept, and should be incorporated into an extended similarity framework. The additional theoretical background for this approach is given in the companion paper by Kitaigorodskii (1988).

Justification for this new framework will be based on the vertically-integrated turbulent kinetic energy balance. The theory will be tested with data from a high-latitude field experiment carried out over the frozen Baltic Sea (Joffre, 1981) where forced convection was the main driving factor. Because the growth of the ABL against background stratification is a very general phenomenon, it is expected that this approach should apply to a wide range of conditions except for pure convective cases and for very stable cases when turbulence is intermittent and breaking of internal waves occur. In our search for universality, we include low-latitude data from the Wangara experiment and also overwater mid-latitude data from the JASIN experiment.

2. The data

2.1. The ICE-77 experiment

An extensive field experiment (ICE-77) carried out over the sea ice fields of the Bothnian Bay between Finland and Sweden (64°30'N, 23°E) during a period of about three weeks in March and April, 1977, provided a large amount of observation data on the ABL. During the experiment, R/V Aranda of the Institute of Marine Research was moored to an ice-floe and then allowed to drift along with the floe. The field experiment was conducted in 2 phases: one between 26 and 31 March and one between 5 and 13 April. Both ice floes had about the same oval shape and size with a mean diameter of about 2 km. They were separated from adjacent floes by pressure ridges with a mean sail height of 30–50 cm. The snow cover was smooth with some undulations here and there.

2.2. Computation of fluxes

The surface layer data were obtained from a 10.2 m high mast with five transverse booms carrying cup anemometers on one side and platinum temperature sensors on the other. The output of these sensors was registered on magnetic tape. The wind data consisted of 10-min averaged runs, whereas temperature data were instantaneous values. Fitting the profiles with the universal functions of the Monin-Obukhov similarity theory φ_m (dimensionless wind shear) and φ_h (dimensionless temperature gradient) allowed us to compute the friction velocity u_* and the surface temperature flux Q_s. The best fit was obtained with $\varphi_m = 1 + 6.7\xi$ and $\varphi_h = 1 + 5.5\xi$ under stable conditions, and with $\varphi_m = (1 - 9\xi)^{-1/4}$ and $\varphi_h = (1 - 5\xi)^{-1/2}$ under unstable conditions, where $\xi = z/L_*$ is the stability parameter and $L_* = -u_*^3/g\beta\kappa Q_s$ is the Monin-Obukhov length scale ($\kappa = 0.4$ is the Karman constant and $g\beta$ the buoyancy parameter). The details of the computation can be found in Joffre (1982). The mean value of the roughness parameter z_0 was 0.04 cm. However, if the form drag due to pressure ridges and hummocks in the ice field is taken into account, the overall roughness length increases to 0.15–0.4 cm with a marked dependence on thermal stability but a large uncertainty in this value (Joffre, 1983).

Figs. 1 and 2 represent the time variation of u_* and Q_s for the periods analysed in this paper. We note that u_* is on average 0.15 m/s while Q_s does not show a marked diurnal cycle at this time of year. Under unstable conditions the ratio $h/|L_*|$ is less than 5 for 75% of the cases, but under stable conditions only 30% of the profiles have such weak buoyancy conditions.

2.3. The height of the ABL

The structure of the whole ABL was studied using low-level radiosondes (type Vaisala RS 17) and numerous pibals up to a minimum of 500 m. All these profiles were constructed from observations every 10 s, thus giving a vertical resolution of about 25 m. The radiosonde ascents were performed at intervals varying from 1.5 to 3 h, giving a total of 28 temperature-humidity-wind profiles. The pibal profilings were performed at regular intervals throughout the day (every 90 min), giving 80 additional wind profiles.

The inaccuracies inherent in the pibal measurements, e.g., their see-saw aspect, due to individual eddies and to the sensitivity of the computed wind to small errors in the observed angles, were smoothed by computing the velocity V at 10 s intervals over layers corresponding to 20 s in thickness.

The ABL height h is a central parameter in both theoretical and application studies. In the

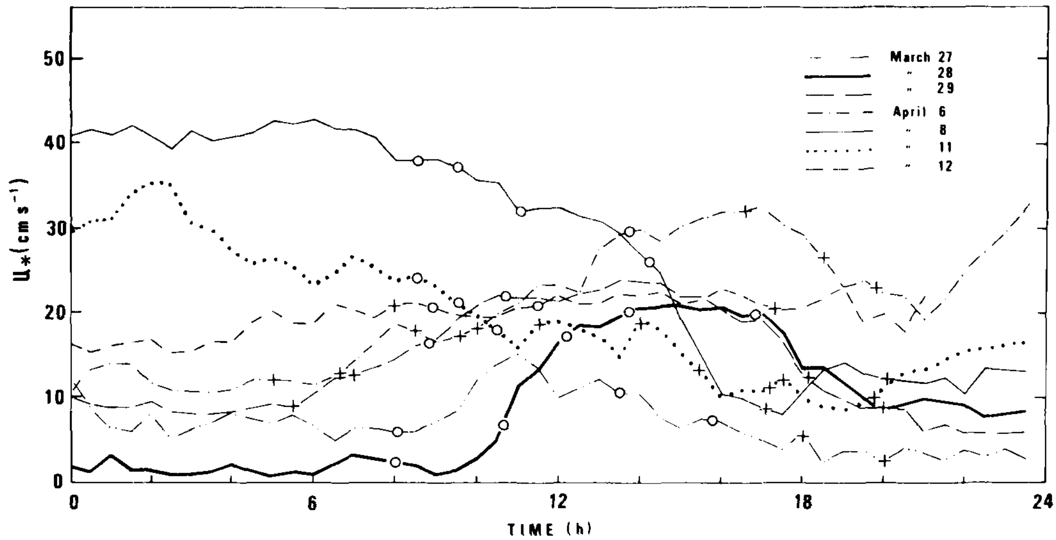

Fig. 1. Diurnal variation of the friction velocity for the most important days of the experiment ICE-77 over the frozen Baltic Sea. Open circles indicate the times of radio/pilot soundings under unstable conditions, while crosses are for soundings under stable conditions.

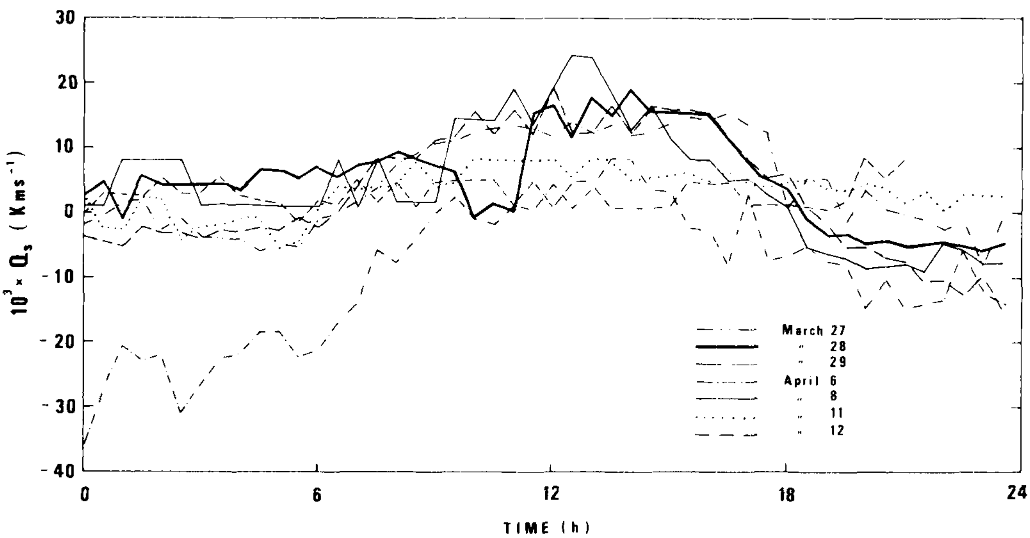

Fig. 2. Same as in Fig. 1 but for the heat flux.

absence of turbulence profiles or SODAR-profiling, this height was determined from inspection of the mean profiles as did, for instance, Melgarejo and Deardorff (1974) for the Wangara data. The height of the inversion base marked the top of the unstable ABL; in fact, the temperature jump was generally small, and to infer h, turning points in the velocity profiles were also considered. For the stable ABL, the layer of significant velocity or directional shear (positive or negative) corresponded to the top of the ABL. In the stable cases, the estimated h was generally lower than the top of the surface inversion, which is determined by both radiative and turbulent

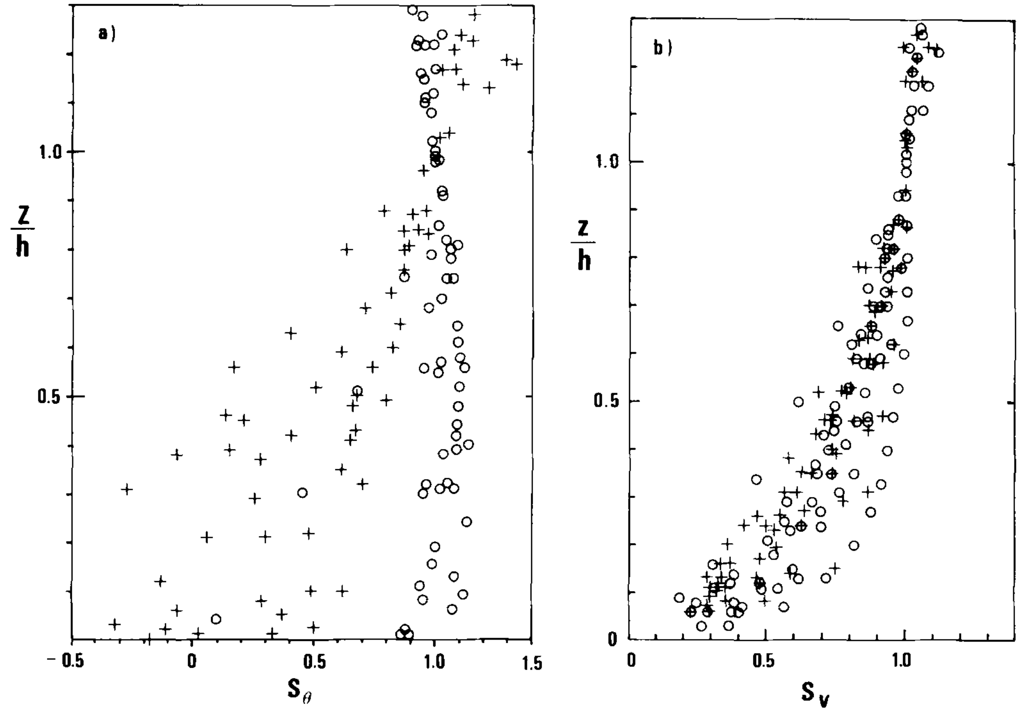

Fig. 3. Dimensionless height dependence of (a) the normalized vertically-averaged potential temperature profiles (b) the normalized vertically-averaged wind velocity for unstable conditions (open circles) and stable conditions (crosses) during ICE-77.

cooling (Garratt and Brost, 1981). Only cases with $\partial h/\partial t \geq 0$ will be considered here, but a few cases for which $\partial h/\partial t$ was unknown were also included.

2.4. *Mean structure of the ABL over sea ice*

We look at the normalized profiles of wind velocity V and virtual potential temperature Θ_v defined as

$$S_r = \frac{\langle r(z)\rangle - r_s}{\langle r_h\rangle - r_s}, \tag{1}$$

where $r = V$ or Θ_v, the subscript s refers to surface values ($V_s = 0$ and $\Theta_{vs} = \Theta_v(z_0)$) and the bracketed terms are vertically-averaged quantities from the surface up to level z or h (see Appendix B). These smoothed profiles are shown here because actual profiles were more erratic and depended on the choice of the lowest level. Nevertheless, both type of profiles were qualitatively similar. We see in Fig. 3a that the dimensionless profile $S_\Theta(z/h)$ is equal to unity through nearly the whole of the depth of the ABL under unstable conditions, whereas S_Θ increases with height under stable conditions. For the wind profiles, on the other hand, no distinction between stability cases was possible and S_V increases from 0 to 1 through the ABL (Fig. 3b). Thus, we find an approximate self-similar behaviour of the wind profiles, independent of time. The profiles are generally not mixed but it is clear that there are situations when mixing is intensive so that, for the sake of generality, we shall include additional data from other sources.

2.5. *Additional data*

Since our data were used for a similarity classification of ABL heights based on a subjective determination, we have incorporated in this paper data from the Wangara experiment (Clarke et al., 1971) which present an independent determination of h values. We have used here the value of h given by Melgarejo and Deardorff (1974) using their estimate h_u from wind profiles for stable cases. Momentum and heat fluxes at the surface were taken from the revised values by Hicks (1981) which better takes into account overall roughness conditions. The background stratification $\gamma = \partial\Theta/\partial z$ was determined from potential temperature profiles between h and $h + 300$ m. Uncertain cases with γ changing sign were deleted, leaving 32 stable profiles and 17 unstable ones. No other criterion was used for selecting the data because we think that the validity of the theoretical approach must be checked against all available data and also because in practice it is nearly impossible to distinguish between the case of the ABL growth in presence of stable stratification and the pure convectively driven ABL.

Additionally, we incorporated the North Sea and Atlantic Ocean data of Nicholls and Readings (1979) and the JASIN data over the North Atlantic from Nicholls (1985), which described the marine type of ABL having a slightly unstable structure $(-h/L_* \approx 5)$ but often a capping cloud deck also. Thus, these three sets of data should represent rather different conditions. All required parameters were taken from the corresponding reports, while Dr. Nicholls kindly provided additional information on his measurements. We note also that no attempt has been made here to account for the effect of the large-scale vertical velocity which can be non-negligible under anticyclonic situations.

3. The overall turbulent kinetic energy balance in stratified ABLs

A common approach for studies on ABL dynamics is to reason with bulk quantities integrated over the height of the ABL. The procedure can be found in works like Mahrt and Lenschow (1976), Kitaigorodskii (1979) and Tennekes and Driedonks (1981). Closure via the equation of turbulent kinetic energy (TKE) should be prefered to those based on the eddy-diffusivity concept, since the TKE equation contains all the physics driving the turbulence field. After integration across the ABL and the interfacial layer one can get for the TKE e_t:

$$\langle e_{th}\rangle \frac{\partial h}{\partial t} = P_\tau + P_h + \tfrac{1}{2}h\left[g\beta Q_s - g\beta\Delta\Theta\frac{\partial h}{\partial t}\right] + M_s - M^+ - h\,\langle\varepsilon_h\rangle - \tilde{\varepsilon}\Delta h \quad (2)$$

where

$$\langle\cdot_h\rangle = h^{-1}\int_0^h (.)\,dz, \quad (\tilde{.}) = \Delta h^{-1}\int_h^{h+\Delta h} (.)\,dz.$$

Δh is the thickness of the interfacial layer (inversion layer), M_s is the diffusion of TKE through the surface and M^+ the loss of TKE through radiation of internal waves, ε is the viscous dissipation. The terms P_τ, P_h represent the production of turbulence by shearing stress and interfacial shear respectively, and are defined as

$$P_\tau = u_*^2\, V_\delta \quad (3)$$

$$P_h = \tfrac{1}{2}(\Delta u^2 + \Delta v^2)\frac{\partial h}{\partial t}, \quad (4)$$

where V_δ is the mean wind velocity at $z = \delta$ ($\delta \approx$ height of constant flux layer) and Δu, Δv, and $\Delta\Theta$ are the jumps in velocity and temperature at the top of the ABL, which can be expressed with the help of the momentum and temperature conservation equations. As a general estimate for turbulence mechanical production we can use the following:

$$P_\tau + M_s = mu_*^3, \quad (5)$$

with as a lowest estimate for the constant m

$$m_{\min} \approx V_\delta/u_* \approx \text{const.} = C_f^{-1/2},$$

where C_f is a drag coefficient. Since, as was shown in section 2.4, the wind profile was not totally mixed through the ABL, $m_{\min}$ can be better estimated as $m_{\min} = C_{fg}^{-1/2}$ where C_{fg} is a geostrophic drag coefficient ($C_{fg} < C_f$).

As a further simplification, we can take $M^+ = 0$ and assume also that the interfacial shear production P_h (the PRT mechanism following Pollard et al., 1973) is almost completely balanced locally by viscous dissipation ($P_h \approx \tilde{\varepsilon}\Delta h$). The small term on the left-hand side of (2) is basically needed only to describe entrainment in the asymptotic case of a nonstratified fluid (see Zilitinkevich, 1975; Tennekes, 1975) and can be omitted. Eventually, the simplified form of (2) that we will use is

$$-\tfrac{1}{2}h\,[g\beta\, Q_h + g\beta Q_s] = mu_*^3 - \langle\varepsilon_h\rangle\, h, \quad (6)$$

where $Q_h = -\Delta\Theta\,\partial h/\partial t$ is the entrainment flux. In the following we shall seek for a simple parameterization of Q_h and express the overall dissipation as a factor times u_*^3, the factor being smaller than m. This is a crude approximation but our main interest here is to find a method describing the variability of h rather than to parameterize the TKE equation.

In order to parameterize the entrainment heat flux $Q_h = -\Delta\Theta\, \partial h/\partial t$, we shall neglect the strong assumption of discontinuity in temperature and using the fact that $\partial h/\partial t = k\ w_m$ and $\Delta\Theta = \Delta h \partial\Theta/\partial z$, we can simply write that

$$Q_h = -\Delta\Theta \frac{\partial h}{\partial t} = -K_h \frac{\partial \Theta}{\partial z} = -K_h \gamma. \tag{7}$$

$K_h = k w_m \Delta h$ is an effective turbulent diffusivity responsible for the overall entrainment process, where w_m is an appropriate velocity scale for vertical turbulent mixing processes leading to ABL growth, and k a numerical constant (not necessarily equal to 0.4), but not too different from unity. Following the idea of overall parameterization (Kitaigorodskii, 1988) according to which entrainment does not have its own characteristic scales, we shall use h instead of Δh as the relevant scale, appealing also to the fact that these two depths are not independent (Deardorff et al., 1980). Then, we will have

$$K_h = k w_m\, h \tag{8}$$

In *unstable* stratification, an additional velocity scale $w_* = (g\beta Q_s h)^{1/3}$ can be constructed and therefore we can write for w_m a general expression of the form

$$w_m = u_*\ \psi(w_*/u_*). \tag{9}$$

The simplest interpolation formula for $\psi(w_*/u_*)$ could be

$$\psi(w_*/u_*) = a_0 + a_1\ w_*/u_* \tag{10}$$

where a_0 and a_1 are constants, such that

$$w_m = a_0\, u_* + a_1\, w_*. \tag{11}$$

The parameterization of entrainment fluxes according to eqs. (7–10) needs some further explanation. Usually, mixed layer models (e.g., Tennekes, 1973) couple eq. (6) together with an expression for the jump $\Delta\Theta(t)$ derived from the heat balance:

$$h\Delta\Theta - h_0\, \Delta\Theta_0 = \tfrac{1}{2}(h^2 - h_0^2) - \int_0^t Q_s(t')\, dt'.$$

This enables one to predict the time evolution of both $h(t)$ and $\Delta\Theta(t)$ once their initial values h_0 and $\Delta\Theta_0$ are known. This obviously requires knowledge of the entrainment rate $u_e = \partial h/\partial t$ (see eq. 6). Laboratory studies (see review in Kitaigorodskii, 1979) basically confirm the fact that the variability of the entrainment rate can be described using overall characteristics of the turbulent boundary layer such as, for instance, the overall Richardson number $\mathrm{Ri}_m = g\beta h\ \Delta\Theta/w_m^2$ (Kitaigorodskii, 1979). This justifies the choice of h as an overall length scale for K_h in (8). Such parameterization for u_e reduces the problem to the solution of only one time-dependent equation (8) together with (6), where $\Delta\Theta$ is a function of all governing parameters (h, u_*, Q_s). As was mentioned before, the assumption of discontinuity in temperature is too strong, and without losing any generality in the derivation of (6) and (8), we can assume the existence of a so-called turbulent entrainment layer or interfacial layer, having a finite thickness Δh. The existence of the finite layer Δh was explicit in the TKE budget equation (2) with the appearance of the term $\tilde{\varepsilon}\Delta h$, which was assumed to be balanced by local shear production inside Δh. Even laboratory studies demonstrate that Δh can be a non-negligible fraction of and proportional to h (Deardorff et al., 1980).

In the atmosphere as well as in the seasonal thermocline (Kitaigorodskii, 1973), it is very difficult to distinguish between the background stratification in the free atmosphere (or below the active seasonal layer in the ocean) and the temperature stratification in the supposedly transitional layer between the well-mixed region of the ABL and the free atmosphere. Therefore, we have decided to use the background stratification $\gamma = \partial\Theta/\partial z$, determined from temperature profiles between h and $h + 300$ m, as a representative value of temperature stratification in the transitional layer. Although the temperature jump in the interfacial layer might be far larger than γ in the overlying free atmosphere we address here the question of the overall treatment of the ABL behaviour (see Kitaigorodskii, 1988).

Naturally, γ, as all other parameters, can depend parametrically on time, but since we are interested in finding a method describing the variability of h, we can assume that in quasi-stationary and quasi-horizontally homogeneous situations, h has adjusted to the local values of Q_s, u_* and γ (more generally to f also), although they all may be variable in time and space, i.e. depend parametrically on time and space. This approach allows us to consider the problem of the ABL height scaling in the framework of the overall TKE balance (6) only.

It appears now that the overall viscous dissipation $\langle \varepsilon_h \rangle h$ is the only unknown for a prediction of h, provided surface fluxes u_*^2 and Q_s and an equation for $\Delta\Theta$ are given. The most detailed parameterization of $\langle \varepsilon_h \rangle h$ was proposed by Garnich and Kitaigorodskii (1977, 1978), (see the review by Kitaigorodskii, 1979). However, it relied completely on the results of laboratory experiments on entrainment in stratified fluids, which still have many deficiencies. An elegant method for parameterization of the dissipation was proposed by Resnyansky (1975), but his approach was limited by the assumption that the growth of the mixed layer occurs in an initially homogeneous fluid. Therefore, without the surface buoyancy flux, mixed layers in his model will inevitably reach the Ekman height u_*/f, whereas in stable or unstable conditions (in terms of surface buoyancy flux) they can depend also on the Monin-Obukhov length L_*. When we emphasize here the role of the *stable background stratification* (N) for the growth of turbulent boundary layers according to our schemes for the entrainment flux, the parameterization of the dissipation present enormous difficulties.

It is clear that under the same internal conditions (u_*, f and Q_s) the dissipation in mixed layers under consideration must be larger than in stratified Ekman boundary layers, since mixed layers cannot grow up to the Ekman height. Therefore, in search for the *maximum* height of the ABL in presence of an imposed stable stratification, it is logical to consider its growth under the conditions of *minimum* dissipation. This is a useful principle anyway, and the stratified Ekman boundary layer (of Monin-Kazanski type) is an example of such a system.

Since we are looking for an equilibrium height solution, we can assume that at any time the ABL turbulence regime is in a quasi-equilibrium state (time enters only parametrically) and then, it is natural to assume that in the asymptotic case when $N/f \gg 1$ the magnitude of the minimum dissipation can be expressed as

$$\langle \varepsilon_h \rangle h = F(u_*, g\beta Q_s, f) = u_*^3\,\Phi(L_E/L_*), \qquad (12)$$

where $L_E = u_*/f$ is the Ekman length (f is the Coriolis parameter), L_* is the Monin-Obukhov length and the ratio $\mu_0 = L_E/L_*$ is the stability parameter of the Monin-Kazanski similarity theory. Other parameters (h and N) could have been introduced in (12) but since we are looking for the maximum ABL height minimizing the dissipation Φ, this will correspond to maximum magnitude of N, itself implying large values of the ratio N/f, what is fulfilled in practice.

For the *neutral* case ($|Q_s| \to 0$) this leads from eq. (6) to

$$\Phi = \text{const.} = m_0 < m. \qquad (13)$$

For *stable* stratification ($Q_s < 0$ or $\mu_0 > 0$) we would assume that

$$\Phi(\mu_0) = \text{const.} = m_1 < m \quad \text{for } \mu_0 \to +\infty. \qquad (14)$$

For *unstable* stratification ($Q_s > 0$ or $\mu_0 < 0$), the situation is not as simple. Because most of the data which we analysed are by and large controlled by both type of turbulence production, we do not need to consider the free convection regime for dissipation, but rather can limit ourselves to the case of convection with a surface shear layer, so that we can again assume $\langle \varepsilon_h \rangle h$ to be independent of rotation, leading to

$$\Phi(\mu_0) = \text{const.} = m_2 \quad \text{for } |\mu_0| \gg 1. \qquad (15)$$

Our assumption of constant m_0, m_1 and m_2 is based on the asymptotic behaviour of the function $\Phi(\mu_0)$.

Since the ratio of the entrainment flux Q_h to the surface heat flux Q_s in the pure convective regime cannot exceed one (see e.g., the estimates of Q_h/Q_s in Zilitinkevich, 1975) this means that for conditions described in Section 3, we cannot assume that $m_2 < m$ for a mechanically-driven ABL, when $Q_s > 0$.

Our parameterization of dissipation becomes finally like the traditional expression with overall dissipation = factor × u_*^3, but with one exception: we distinguish between the values of the factor of proportionality in different conditions in terms of surface buoyancy fluxes Q_s. Thus, it is a little bit more general approach that the pure empirical parameterization of dissipation with only one mixing efficiency m (see review of Kitaigorodskii, 1979). This formulation completes the closure for eq. (6).

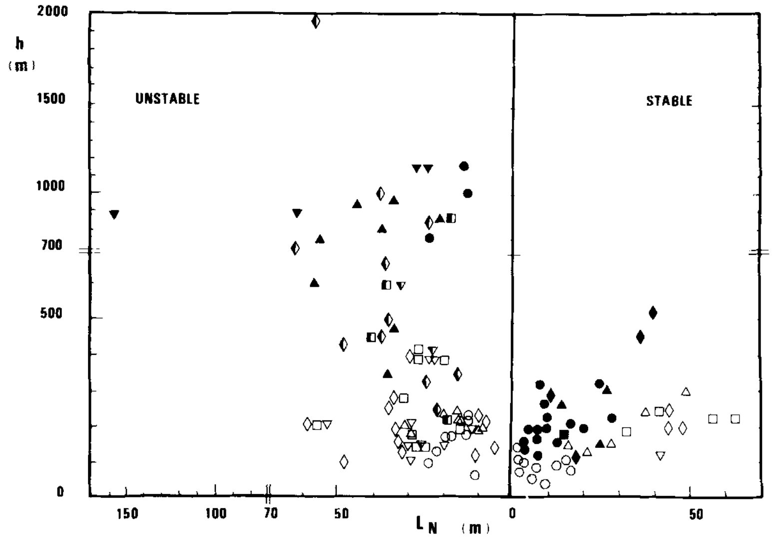

Fig. 4. Dependence of the ABL height h on the scale $L_N = u_*/N$ for stable cases (right-hand side) and unstable cases (left-hand side). The data are classified according to the magnitude of L_*: (○) $L_* \leq 20$; (△) $20 < L_* \leq 50$; (▽) $50 < L_* \leq 100$; (□) $100 < L_* \leq 200$; (◇) $L_* > 200$ m. Open symbols correspond to the ICE-77 data, full symbols to the Wangara data and the half-open symbols to the JASIN data. Note that the scale changes on the abscissa when $L_N > 70$ and on the ordinate when $h > 700$.

4. ABL height scaling

It is convenient in what follows to consider separately the cases of neutral, stable and unstable stratification, following the traditional classification of stationary Ekman layers.

4.1. Neutral case

We shall define the neutral case here as a limiting case when the underlying earth's surface is neither a source of atmospheric heat nor a sink. It corresponds to the case $|Q_s| \to 0$. This of course does not mean that the real stratification conditions are neutral within the ABL, because of the existence of the entrainment flux Q_h. This latter basically produces a stable stratification throughout the whole ABL. Further, if $Q_s < 0$, i.e., the earth acts as a sink of atmospheric heat, the stratification in the ABL will be more stable (with the same Q_h) than in the limiting case when $Q_s \to 0$. Conversely, in the case $Q_s > 0$, i.e., when the earth's surface heats the atmosphere, the stratification in the ABL will be less stable than in the asymptotic case when $Q_s \to 0$ (again with the same Q_h).

In the framework of the system of eqs. (6)–(15), the limiting case $Q_s \to 0$ leads to

$$k a_0\, u_*\, h^2\, N^2 = 2(m - m_0)\, u_*^3, \tag{16}$$

or

$$h = b L_N, \tag{17}$$

where $L_N = u_*/N$, $N = (g\beta\gamma)^{1/2}$ is the Brunt-Väisälä frequency and $b = [2(m - m_0)/k a_0]^{1/2} = \text{const}$. Thus, the scale L_N characterizes the scale of the ABL.

The physical meaning of L_N in (17) is clear: it corresponds to the scale of a well-mixed region developed by upwards diffusion of turbulent energy in the presence of a background stratification N. The limiting scale L_N for the most stable conditions appears as a direct consequence of the existence of a limiting value for the flux Richardson number R_f, based in this case on the entrainment flux Q_h

$$R_f = \frac{g\beta Q_h}{u_*^2\, \mathrm{d}V/\mathrm{d}z} = \frac{k a_0\, u_*\, N^2\, h^2}{m u_*^3} = R_{fcr}. \tag{18}$$

This yields

$$h = (m R_{fcr}/k a_0)^{1/2}\, L_N = b'\, L_N. \tag{19}$$

Taking typical values for m, k and a_0 (see Appendix A) and R_{fcr} in the range 0.25–1, gives $b' \approx 4 - 13$. This is in reasonable agreement with observations (see Fig. 4). Comparing eq. (17) to eq. (19) shows that $m_0 = m(1 - R_{fcr})$ and consequently the *overall* dissipation is a smaller fraction of the *overall* shear production in very stable stratification. Note that if we use the factor $(2\pi)^{-1}$ to express N in s^{-1}, b' is of order unity.

4.2. *Stable stratification* ($Q_s < 0$)

If $Q_s < 0$, $w_* = 0$ and, eq. (6) can be rewritten as

$$k a_0 u_* h^2 N^2 - g\beta Q_s h = 2(m - m_1) u_*^3. \tag{20}$$

Here also, following the idea of overall parameterization, mixing at the top of the ABL was assumed to be represented by the surface scale $a_0 u_*$. In nondimensional form (20) turns to

$$a' h_*^2 \mu_N^{-2} + h_* = m', \tag{21}$$

where $h_* = h/L_*$, $\mu_N = L_N/L_* > 0$. The coefficients $a' = k\kappa a_0$ and $m' = 2(m - m_1)\kappa$ are positive constants. The important length scales here are only L_* and L_N, and the nondimensional ABL height h_* depends only on μ_N.

It follows from the conditions $N \to \infty$ (i.e., $\mu_N \to 0$) that

$$h_* \to (m'/a')^{1/2} \mu_N \quad \text{or} \quad h = (m'/a')^{1/2} L_N. \tag{22}$$

Of course it is debatable whether entrainment in such a situation will definitively cease at this height. The recent laboratory experiments by Fernando and Long (1985) do not show this tendency. However, in geophysical situations, a rather strong stable stratification in the atmosphere will certainly prevent the effective growth of the mixed layer. Thus, we can accept the dependence of h, the height of the ABL, on L_* and L_N, as was discussed in subsection 4.1.

If there is a nonzero surface heat flux Q_s then, for large enough values of μ_N ($N \to 0$), entrainment can in practice cease at a level independent of the initial stratification, and

$$h_* = \text{const.} = m' \quad \text{or} \quad h = m' L_* \quad (\text{for } \mu_N \to \infty). \tag{23}$$

Kitaigorodskii (1960) found a similar relationship on the basis of oceanic measurements with $m' \approx 2$. Resnyansky (1975) for his part arrived at

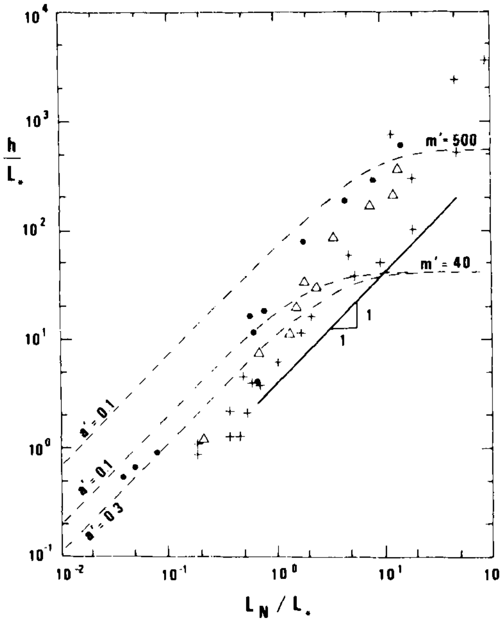

Fig. 5. Dependence of the dimensionless height $h_* = h/L_*$ on the stability parameter $\mu_N = L_N/L_*$ under stable conditions illustrating the function f_+. The dashed lines correspond to solutions of eq. (27) with different values of a' and m'. (+) $N/f < 60$, (△) $60 < N/f < 115$ and (●) $N/f > 115$. The data are those of ICE-77 and Wangara.

a maximum depth expression $h \approx 12\ L_*$. Thus, the proper scaling for the stably stratified ABL is simply

$$h_* = f_+(\mu_N), \tag{24}$$

where the function f_+ has the doubly asymptotic behaviour

$$f_+(\mu_N) = \alpha\mu_N \quad \text{for} \quad \mu_N \to 0, \tag{25}$$

with $\alpha = (m'/a')^{1/2} = \text{const.}$, and

$$f_+(\mu_N) = \text{const.} = m' \quad \text{for} \quad \mu_N \to +\infty. \tag{26}$$

In the general case, the solution of (21) gives a scale h_*^{st} for the stable ABL defined as

$$h_*^{st} = \frac{-1 + \sqrt{1 + 4a' m' \mu_N^{-2}}}{2a' \mu_N^{-2}}, \tag{27}$$

Now the important question is: how does this similarity framework describe real data, in spite of the many simplifying assumptions made in the derivation?

We present in Fig. 5 the function (24) with the results of Joffre (1981) and those of the Wangara field experiment (Clarke et al., 1971). It shows that there is a definite relationship between h_* and μ_N according to (24). Moreover, taking reasonable estimates for the constants a' and m' in eq. (22), i.e.,

$$a' = k\kappa a_0 \approx 0.1 - 0.3 \quad \text{and} \quad m' \approx 40, \tag{28}$$

(see Appendix A for the derivation of these constants), we obtain a rather good fit of the data for $\mu_N < 5$, but increasingly bad with increasing μ_N. Note that we have included only cases with $\partial h/\partial t \geq 0$ since the case of the collapse of the stable ABL would imply different physical processes and scales. It seems that (27) is a good approximation except for large values of μ_N, where the data can be fitted only with unrealistically large values of m' (≈ 500). The question of spurious correlation effects in a graph like Fig. 5 will be addressed at the end of Subsect. 4.3.

For larger values of μ_N ($\mu_N > 5$), we probably need much larger values for production of TKE. Naturally, due to the crudeness of our parameterization of the overall turbulent energy balance (6), and especially the parameterization of dissipation (7–10), we have avoided a description of the variability of h_* with $\mu_0 = L_E/L_*$, which can be implicitly present by assuming that both a' and m' depend parametrically on μ_0. It must be noticed, however, that under strong stability conditions, all turbulent fluxes (u_* and Q_s), as well as the ABL height h, are poorly defined.

It remains to be seen whether such a procedure can sufficiently improve the description of the existing empirical data presented here in Fig. 5, but it is more or less clear that by including the PRT mechanism for larger values of μ_N we can improve the parameterization of the overall TKE balance. In Fig. 5, we have differentiated the data according to $L_E/L_N = N/f$, in order to include the length L_E in the description of the data. The figure shows that N/f helps to describe the scatter for small and moderate μ_N, with h/L_* increasing with increasing N/f values at a given μ_N value.

4.3. *Unstable stratification ($Q_s > 0$)*

In the unstable case, eq. (6) can be written in nondimensional form as

$$\{a' + a''|h_*|^{1/3}\}\, h_*^2\, \mu_N^{-2} - |h_*| = m'', \tag{29}$$

where $a'' = ka_1\kappa^{2/3}$ and $m'' = 2\ (m - m_2)\ \kappa >$ or <0. Since the majority of the experimental data included corresponds to a mechanically-driven ABL, we limit our analysis here by considering only the case $m'' > 0$. We can also simplify things by assuming that the entrainment process is dominated by the dynamical (but not convective) velocity scale, which requires that at least

$$a' > a''\, h_*^{1/3}. \tag{30}$$

For $h_* \approx 100$, this leads approximately to $a' > 5a''$, which is not unreasonable. Thus, the scale h_*^{unst} for the unstable ABL defined as

$$|h_*^{\text{unst}}| = \frac{1 + \sqrt{1 + 4a'\, m''\, \mu_N^{-2}}}{2a'\, \mu_N^{-2}} \tag{31}$$

will not really differ from the scale h_*^{st} (Eq. 27) of the stable ABL for $|\mu_N| < 1$.

Thus the proper scaling for the unstably stratified ABL is simply

$$|h_*| = f_-(|\mu_N|). \tag{32}$$

In order to define the asymptotic properties of this function, one needs to consider in more detail the overall balance (29). Within the framework of eq. (29) we are allowed to consider the free convection regime, defined as a limit for $u_* \to 0$. It leads to a scale for the convectively-driven mixed layer

$$h = dL_c = (a'')^{-3/4}\, (g\beta\kappa Q_s/N^3)^{1/2} \tag{33}$$

The physical meaning of $L_c = (g\beta\kappa Q_s/N^3)^{1/2}$ is clear from eq. (29): it corresponds to the scale of the mixed layer developed under convective mixing in an initially linearly stratified fluid ($Q_s = 0$; $L_N \to 0$, $|\mu_N| \to \infty$). In terms of the universal function $f_-(|\mu_N|)$ (see Eq. 32), it can be written as

$$f_- \to (a'')^{-3/4}\, |\mu_N|^{3/2} \quad \text{for} \quad |\mu_N| \to \infty. \tag{34}$$

We present in Fig. 6 a comparison of eq. (31) with different values of a' against the same observational data as in the stable case, and additionally against data gathered over the North Sea and the Atlantic Ocean (Nicholls and Readings, 1979; Nicholls, 1985). In fact, it shows that the asymptotic situation (34) is not yet achieved in the range of μ_N values of our experimental data. For smaller values of $|\mu_N|$ we can

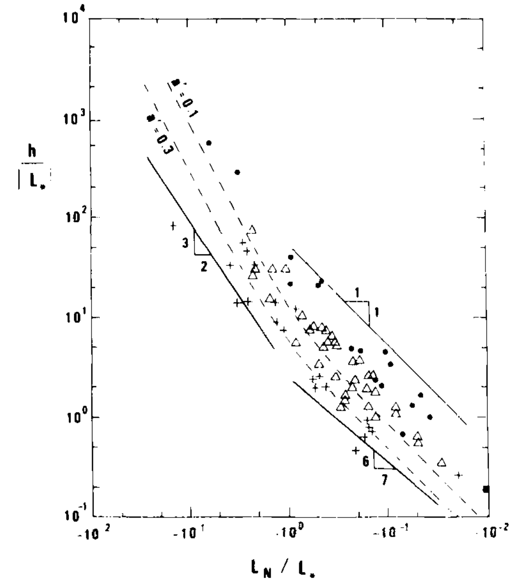

Fig. 6. Dependence of the dimensionless height $h_* = h/L_*$ on the stability parameter $\mu_N = L_N/L_*$ under unstable conditions illustrating the function f_-. The two dashed lines correspond to solutions of eq. (31) with different values of a'. The different symbols depict different values of N/f (see Fig. 5). The data shown are those of ICE-77, Wangara and JASIN.

consider a regime that we may call "convection with shear", when two conditions are fulfilled: $a' < a''|h_*|^{1/3}$ and also $m'' \gg |h_*|$. Then, the turbulence energy balance can be reduced to another simple form:

$$a''|h_*|^{7/3}\,\mu_N^{-2} = m'' > 0, \tag{35}$$

so that

$$f_-(|\mu_N|) = (m''/a'')^{3/7}\,|\mu_N|^{6/7} \quad \text{for} \quad |\mu_N| < 1. \tag{36}$$

The slope 6/7 is not very different, either, from the observations in Fig. 6. Here again the differentiation according to the scale ratio L_E/L_N helps to describe the internal scatter.

On the basis of Fig. 4, we have discussed the asymmetrical behaviour of h in unstable and stable conditions, pointing out that $h^{unst} > h^{st}$ due to the additional production source. However, putting Figs. 5 and 6 side by side (which, by the way, resembles the famous Monin-Obukhov's (1954) "bird" picture), we notice that the increase of $|h_*|$ versus $|\mu_N|$ is rather symmetric. This could mean that for the analyzed data, the regime in which Q_s is an important additional source of TKE has not yet been reached, and that only shear production and entrainment fluxes contribute to the energy budget. This can be checked by inspecting the ratio of the entrainment flux Q_h to the surface heat flux Q_s. Using parameterization (11) yields

Table 1. *Average values of the ratio $Q_h/|Q_s|$ for different values of $|\mu_N|$.*

$|\mu_N|$	10^{-2}	10^{-1}	10^0	10^1	5×10^1
stable case	—	20	2	0.3	0.08
unstable case	200	40	2	2	—

$$Q_h/|Q_s| = a'|h_*|\mu_N^{-2}. \tag{37}$$

This ratio can be estimated using average values in the graphs of Figs. 5 and 6. The results are shown in Table 1. It appears that $Q_h \gg |Q_s|$ for $|\mu_N| < 1$ in both stable and unstable conditions. For conditions corresponding to $|\mu_N| > 1$, the heat flux ratio of (37) keeps its large value only under unstable conditions. This means that these empirical data are still in the range where the surface heating-induced convection can be neglected (i.e., the term in w_* is deleted). For the stable case, in contrast, the ratio $Q_h/|Q_s|$ becomes smaller than unity when $\mu_N > 1$, and top-entrainment effects are of minor importance.

It must be remarked that the results shown in Figs. 5 and 6 can be affected by the notorious spurious relationship effect, since both abscissa and ordinate are normalized by L_*. Furthermore, L_* varies relatively more widely than h or L_N (2 to 3 times more). These lengths include as independent parameters: u_*, h, N and $T_* = -Q_s/u_*$. In order to eliminate the dependence in u_*, we plot the quantity hL_*/L_E^2 as a function of L_N/L_*. These provide a well-defined relationship in both stability cases, with $hL_*/L_E^2 \approx 0.002$ (L_*/L_N), which can in its turn be converted into $h/L_* = 0.002$ (L_N/L_*) $(N/f)^2$, i.e., the observed dependence in Figs. 5, 6. Now eliminating the spurious correlation due to T_* by plotting h/L_N against $\mu_0 = L_E/L_*$ yields (with some scatter): $h/L_* \approx 12.5 + 0.01\,\mu_0$ under stable conditions, and $h/L_* \approx 12.5 + 0.045\,\mu_0$ under unstable conditions. These results also lead to $h/L_* \approx 12.5$ (L_N/L_*), where the proportionality coefficient becomes dependent on μ_0 when $\mu_0 > 100$. In conclusion, although spurious correlation effects contribute somewhat to the quality of the plot in Figs. 5, 6, the displayed results have a sound physical basis which is supported by observations.

5. Conclusion

We can conclude that existing data on the evolution of ABLs in both stable ($Q_s < 0$) and unstable ($Q_s > 0$) conditions are not inconsistent with the assumption that the balance between entrainment and surface heat flux can be parameterized in the simple form (6–15). Moreover, it appears that classical ground-based measurements of turbulent fluxes do not always provide a realistic description of the important contributions influencing the dynamics of the whole ABL. Rather, background stratification through the parameter N plays a very important role. This leads to the inclusion of the length scale $L_N = u_*/N$ into the similarity description of the ABL height.

The approach was tested against very different sets of data but should be checked further in order to assess more accurately the extent of application of the method. As was previously mentioned, more data will be also necessary to investigate the possible variability of the growing ABL with the Monin-Kazanski parameter μ_0.

6. Acknowledgements

One of us (SAK) would like to acknowledge support from the Finnish Meteorological Institute. The ICE-77 data were obtained by the second author (SMJ) while he was affiliated to the Finnish Institute of Marine Research (IMR); we are grateful to the IMR for permission to use these data. Our special thanks is due to Ms. Tarja Savunen for technical assistance. We are also grateful to R. Clarke, B. Hicks and S. Nicholls for kindly providing their data. SMJ was supported by the Nordic Council of Ministers.

7. Appendix A

7.1. Determination of the constant m

The factor m (eq. 5) is inversely proportional to the square root of a drag coefficient. In order to account implicitly for the shear throughout the ABL it is more convenient to take it as a geostrophic drag coefficient m_g. During the ICE-77 experiment m_g varied between 30 (unstable conditions), 45 (neutral conditions) and 100 (stable conditions).

7.2. Determination of k and a′

Wyngaard and Brost (1984) fitted the eddy diffusivity K_t resulting from top-down mixing by the expression

$$K_t = w_* hz^+ (1 - z^+)^{3/2}, \tag{A1}$$

where z^+ is the dimensionless height z/h. Since we are dealing with an overall model, we integrate expression (A1) between h and $\frac{1}{2}h$, the layer in which entrainment effects are likely to be observed. This yields

$$K_t = \frac{2}{h}\int_{\frac{1}{2}h}^{h} K_t(z)\,\mathrm{d}z = 0.0.9\ w_*\ h, \tag{A2}$$

so that $k \approx 0.1$. On the other hand, Mahrt and André (1983) implied that in a near-neutral ABL, $K \sim 0.07\ u_*\ h$ at $z^+ = 0.5$, thus implying $k \approx 0.25$. The parameterization (8) states that $K_h = khw_m$. Since $w_m = u_*\ [25 + (w_*/u_*)^3]^{1/3}$ (Driedonks and Tennekes, 1984), then,

$$a' = a_0\ k\kappa \approx 0.1\text{–}0.3.$$

7.3. Determination of m_1 and m'

Under stable conditions Brost and Wyngaard (1978) found that their model's dissipation is well fitted by

$$\frac{\varepsilon\kappa h}{u_*^3} = \frac{(1 + 3.7\ h_*\ z^+)\ (1 - 0.85\ z^+)^{3/2}}{z^+} \tag{A3}$$

Integrating (A3) between the surface and h leads to

$$h\langle\varepsilon_h\rangle = u_*^3\ [3.7\ \mu_0\ h/L_E - 2.8 - 2.5\ \ln(z_0^+)] \tag{A4}$$

where $z_0^+ = z_0/h$ and z_0 is the roughness length. The bracketed term is equivalent to m_1 for large h_* values. According to the ICE-77 and Wangara data $h/L_E \approx 0.1$ and $z_0^+ = 2 \times 10^{-6}$, choosing a maximum $\mu_0 \approx 50$ leads to $m_1 \approx 50$. Consequently, for the constant $m' = 2\ (m - m_1)\ \kappa$ we found

$$m' \approx 40.$$

7.4. Determination of m_2 and m''

According to the results of Caughey and Palmer (1979)

$$h\varepsilon/w_*^3 = 1.5 - 1.15\, z^+. \quad \text{(A5)}$$

Integrating (A5) through the ABL yields

$$h\,\langle\varepsilon_h\rangle = 0.925\, w_*^3.$$

Since $h\langle\varepsilon_h\rangle \to m_2\ u_*^3$, using $(w_*/u_*)^3 = h/\kappa L_*$ leads to $m_2 \approx 23$ with $\mu_0 = 100$ and $h/L_E = 0{\cdot}1$. Consequently

$$m'' = 2\,(m - m_2)\,\kappa \approx 6.$$

8. Appendix B

List of Symbols

a_0	Proportionality coefficient for u_* in the velocity scale w_m expression
a'	$= k\kappa a_0$
a_1	proportionality coefficient for w_* in the velocity scale w_m expression
a''	$= ka_1\kappa^{2/3}$
b, b'	proportionality coefficient between h and L_N (neutral case)
f	Coriolis parameter
f_+, f_-	functions describing the normalized ABL height h/L_* and depending on the parameter $\mu_N = L_N/L_*$, for stable and unstable conditions, respectively
$g\beta$	buoyancy parameter ($= g/T$)
h	ABL height
h_*	dimensionless ABL height ($= h/L_*$)
k	Proportionality coefficient for the effective eddy diffusivity K_h driving entrainment
K_h	effective eddy diffusivity connected to summital entrainment
L_*	Monin-Obukhov length ($= -u_*^3/g\beta\kappa Q_s$)
L_N	background stratification scale ($= u_*/N$)
L_E	Ekman scale ($= u_*/f$)
m	mechanical production of turbulence normalized by u_*^3
m_0	normalized overall viscous dissipation $\Phi = h\langle e_h\rangle/u_*^3$ in neutral conditions
m_1	$= \Phi\ (\mu_0 \to +\infty)$, very stable conditions
m_2	$= \Phi\ (\mu_0 \to -\infty)$, very unstable conditions
m'	$= 2\,(m - m_1)\kappa$
m''	$= 2\,(m - m_2)\kappa$
N	Brunt-Väisälä frequency ($= \sqrt{g\beta\gamma}$)
Q_s	surface temperature flux ($= \overline{T'w'}$)
Q_h	summital entrainment flux ($= (\overline{T'w'})_h$)
T	temperature
T_*	temperature scale ($= -Q_s/u_*$)
u_*	friction velocity
V	wind velocity ($= (u^2 + v^2)^{1/2}$
w_m	velocity scale for the ABL ($= a_0\,u_* + a_1\,w_*$)
w_*	convective velocity scale ($= (g\beta hQ_s)^{1/3}$)
z_0	roughness length
γ	background stratification ($= \partial\Theta/\partial z$ above the ABL)
$\Delta\Theta$	temperature difference across the entrainment layer
Δh	thickness of the entrainment layer
ε	viscous dissipation
Φ	dimensionless viscous dissipation ($= h\langle\varepsilon_h\rangle/u_*^3$)
κ	Karmán constant ($= 0.4$)
μ_0	stability parameter ($= L_E/L_*$)
μ_N	stability parameter ($= L_N/L_*$)

Θ, Θ_v potential temperature and virtual potential temperature
ξ stability parameter in the surface layer ($= z/L_*$)
$\langle \cdot_h \rangle$ vertically-integrated quantity throughout the ABL ($= h^{-1} \int_0^h (.)\, dz$)
$\langle . \rangle$ vertically-integrated quantity ($= z^{-1} \int_0^z (.)\, dz'$)
$(\tilde{.})$ vertically-integrated quantity in the interfacial layer
$(.)_s$ surface values
$(.)_0$ initial values

REFERENCES

Brost, R. A. and Wyngaard, J. C. 1978. A model study of the stably stratified planetary boundary layer. *J. Atmos. Sci. 35*, 1427–1440.

Caughey, S. J. and Palmer, S. G. 1979. Some aspects of turbulence structure through the depth of the convective boundary layer. *Quart. J. R. Met. Soc. 105*, 811–827.

Caughey, S. J., Wyngaard, J. C. and Kaimal J. C. 1979. Turbulence in the evolving stable boundary layer. *J. Atmos. Sci. 36*, 1041–1052.

Clarke, R. H., Dyer, A. J., Brook, R. R., Reid, D. G. and Troup, A. J. 1971. The Wangara experiment: Boundary Layer Data. *Techn. Pap. No. 19*, CSIRO, Division of Meteorological Physics, Aspendale, Australia, 362 pp.

Deardorff, J. W., Willis, G. E. and Stockton B. H. 1980. Laboratory studies of the entrainment zone of a convectively mixed layer. *J. Fluid Mech. 100*, 41–64.

Driedonks, A. G. M. and Tennekes, H. 1984. Entrainment effects in the well-mixed atmospheric boundary layer. *Boundary-layer Meteorol. 30*, 75–105.

Fernando, H. J. S. and Long, R. R. 1985. On the nature of the entrainment interface of a two-layer fluid subjected to zero-mean-shear turbulence. *J. Fluid Mech. 151*, 21–53

Garnich, N. G. and Kitaigorodskii, S. A. 1977. On the rate of deepening of the oceanic mixed layer. *Izv Acad. Sci. USSR, Atmos. Ocean. Phys. 13*, 888–893.

Garnich, N. G. and Kitaigorodskii S. A. 1978. On the theory of the deepening of the upper quasihomogeneous ocean layer owing to the processes of purely wind-induced mixing. *Izv. Acad. Sci. USSR, Atmos. Ocean. Phys. 14*, 748–755.

Garratt, J. R. and Brost, R. A. 1981. Radiative cooling effects within and above the nocturnal boundary layer. *J. Atmos. Sci. 38*, 2730–2746.

Hicks, B. B. 1981. An analysis of Wangara micrometeorology: surface stress, sensible heat, evaporation, and dewfall. *NOAA Techn. Memorandum ERL ARL-104*, 36 pp.

Joffre, S. M. 1981. The physics of the mechanically-driven atmospheric boundary layer as an example of air-sea ice interactions. *Report no. 20*, Dept. Meteorology, Univ. of Helsinki, 75 pp.

Joffre, S. M. 1982. Momentum and heat transfers in the surface layer over a frozen sea. *Boundary-Layer Meteorol. 24*, 211–229.

Joffre, S. M. 1983. Determining the form drag contribution to the total stress of the atmospheric flow over ridged sea ice. *J. Geophys. Res. 88*, 4524–4530.

Kazanski, A. B. and Monin, A. S. 1960. The turbulent regime above the surface atmospheric layer. *Izv. Acad. Sci. Ser. Geofiz. 1*, 165–168.

Kitaigorodskii, S. A. 1960. Calculating the thickness of the wind-induced mixing layer in the ocean. *Izv. Akad. Nauk SSSR., Ser Geof. 3*, 425–431 (English Ed. 284–287).

Kitaigorodskii, S. A., 1973. *The physics of air-sea interaction.*, Israel Prog. Scient. Transl., Jerusalem, pp. 236.

Kitaigorodskii, S. A. 1979. Review of the theories of wind mixed layer deepening. Marine Forecasting. *Proceedings of X Liege Colloquium on Ocean Hydrodynamics*, Elsevier Publ. 4, 1–33.

Kitaigorodskii, S. A. 1988. A note on similarity theory for atmospheric boundary layers in presence of background stable stratification. *Tellus 40A*, 434–438.

Mahrt, L. and André, J. C. 1983. On the stratification of turbulent mixed layers. *J. Geophys. Res. 88*, 2662–2666.

Mahrt, L. and Lenschow, D. H. 1976. Growth dynamics of the convectively mixed-layer. *J. Atmos. Sci. 33*, 41–51.

Melgarejo, J. W. and Deardorff, J. W. 1974. Stability functions for the boundary layer resistance laws based on observed boundary-layer heights. *J. Atmos. Sci. 31*, 1324–1333.

Monin, A. S. and Obukhov, A. M. 1954. Basic laws of turbulent mixing in the surface layer of the atmosphere. *Tr. Geofiz. Inst. Akad Nauk USSR 24 (151)*, 173–187.

Nicholls, S. 1985. The structure of the marine atmospheric boundary layer observed during JASIN. *Quart. J. R. Met. Soc. 111*, 391–426.

Nicholls, S. and C. J. Readings 1979. Aircraft observations of the structure of the lower boundary layer over the sea. *Quart. J. R. Met. Soc. 105*, 785–802.

Nieuwstadt, F. T. M. and Tennekes, H. 1981. A rate equation for the nocturnal boundary-layer height. *J. Atmos. Sci. 38*, 1418–1428.

Niiler, P. P. 1975. Deepening of the wind-mixed layer. *J. Mar. Res. 33*, 405–422.

Pollard, R. T., Rhines, P. B. and Thompson, R. O. R. Y. 1973. The deepening of the wind-mixed layer. *Geophys. Fluid. Dyn. 3*, 381–404.

Resnyansky, Yu. D. 1975. Parameterization of the integral turbulent energy dissipation in the upper quasihomogeneous layer of the ocean. *Izv. Acad. Sci. USSR, Atmos. Ocean. Phys.* 11, 453–457.

Tennekes, H. 1973. A model for the dynamics of the inversion above a convective boundary layer. *J. Atmos. Sci. 30*, 558–567.

Tennekes, H. 1975. Reply to comments on "A model for the dynamics of the inversion above a convective boundary layer". *J. Atmos. Sci. 32*, 992–995.

Tennekes, H. and Driedonks, A. G. M. 1981. Basic entrainment equations for the atmospheric boundary layer. *Boundary-layer Meteorol. 20*, 515–531.

Wyngaard, J. C. and Brost, R. A. 1984. Top-down and bottom-up diffusion of a scalar in the convective boundary layer. *J. Atmos. Sci. 41*, 102–112.

Zeman, O. 1979. Parameterization of the dynamics of stable boundary layers and nocturnal jets. *J. Atmos. Sci. 36*, 792–804.

Zeman, O. and Lumley, J. L. 1976. Modelling buoyancy driven mixed layers. *J. Atmos. Sci. 33*, 1974–1988.

Zeman, O. and Tennekes, H. 1977. Parameterization of the turbulent energy budget at the top of the daytime atmospheric boundary layer. *J. Atmos. Sci. 34*, 111–123.

Zilitinkevich, S. S. 1975. Comments on "A model for the dynamics of the inversion above a convective boundary layer". *J. Atmos. Sci. 32*, 991–995.